

Realizing Universal Majorana Fermionic Quantum Computation

Ya-Jie Wu,¹ Jing He,¹ and Su-Peng Kou^{1,*}

¹*Department of Physics, Beijing Normal University, Beijing 100875, China*

(Dated: March, 2013)

Majorana-fermionic quantum computation (MFQC) was proposed by Bravyi and Kitaev (See Ref.[1]), in which a fault-tolerant (non-topological) quantum computer built from Majorana fermions may be more efficient than that built from distinguishable two-state systems. However, till now people don't know how to realize a MFQC in a physical system. In this paper we proposed a possible realization of MFQC. We find that the end of a line-defect of p-wave superconductor or superfluid on a honeycomb lattice will trap a Majorana zero mode, which will become the starting point of MFQC. Then we show how to manipulate Majorana fermions to do universal MFQC, which possesses unique possibilities for high-level local controllability, individual addressing, and readout of the quantum states of individual constituent elements by using timely cold-atom technology.

Introduction.—Quantum computer makes use of the principles of quantum physics to enhance the computational power beyond what is attainable by a traditional computer. Various designs have been proposed to build a quantum computer, such as manipulating electrons in a quantum dot or phonon in ion traps, cavity quantum electrodynamics, nuclear spin by nuclear magnetic resonance techniques. However, the realization of low decoherence condition in these schemes is a great challenge to achieve a true quantum computer. Because the noise and decoherence are presumably caused by local interactions, people try to avoid them by encoding quantum information non-locally. This leads to so called topologically protected qubit[2–4]. In particular, the topological quantum computation is proposed based on the manipulation of non-Abelian anyons[5–9]. The possible candidates may be the fractional quantum Hall state at filling factor $\nu = 5/2$ in ultra high-mobility samples[10, 11], the two dimensional (2D) chiral $p_x + ip_y$ superconductors[12], and the s-wave-superconductor-topological-insulator systems[13, 14]. Yet, people cannot realize universal quantum computation just by braiding Ising-type non-Abelian anyons. In addition, among these approaches, accurate manipulation of single anyon remains a major difficulty and new techniques are expected to overcome this drawback.

In this paper we turn to an alternative type of fault-tolerant quantum computation - Majorana-fermionic quantum computation (MFQC). Majorana-fermionic quantum computation was proposed by Bravyi and Kitaev[1], in which the qubits are characterized by fermion's parity. A quantum computer built from Majorana fermions may be more efficient than that built from distinguishable two-state systems. Although MFQC is not the topological quantum computation, the quantum information with Majorana fermions also intrinsically immune to decoherence. Thus it is possible to do universal quantum computation by manipulating the two-Majorana-fermion interaction ($\gamma_1\gamma_2$) and the four-

Majorana-fermion interaction ($\gamma_1\gamma_2\gamma_3\gamma_4$). We find that the end of a line-defect of p-wave superconductor (SC) or superfluid (SF) on a honeycomb lattice will trap a Majorana zero mode, which will become the starting point of MFQC[15]. Then we show how to manipulate Majorana fermions to do universal MFQC and also discuss the errors. In the end, we design an experiment scheme for the realization of the p-wave SF in a Bose-Fermi mixture on an optical honeycomb lattice.

P-wave superconductor/superfluid for spinless fermions on honeycomb lattice: We start from a spinless fermion model on a honeycomb lattice with nearest attractive interaction as

$$\hat{H} = -t \sum_{\langle ij \rangle} \hat{c}_i^\dagger \hat{c}_j - t' \sum_{\langle\langle ij \rangle\rangle} \hat{c}_i^\dagger \hat{c}_j + h.c. - \mu \sum_i \hat{n}_i - U \sum_{\langle ij \rangle} \hat{n}_i \hat{n}_j, \quad (1)$$

where t (t') and U denote the strength of nearest (next nearest) neighbor hopping and the nearest neighbor attractive interaction respectively, μ is chemical potential, and $\hat{n}_i = \hat{c}_i^\dagger \hat{c}_i$ denotes the particle number operator.

As increasing the interaction strength, the system turns into a p-wave SC/SF ground state in the region of $3.36t \leq U \leq 7.12t$ for the case of $t' = 0$ at zero temperature[17]. In the limit of $t' \ll t$, the p-wave SF order is still stable. For the p-wave SC/SF, the p-wave pairing order parameter is given as $\Delta_{j,j+\mathbf{a}_1} = \langle \hat{c}_j^\dagger \hat{c}_{j+\mathbf{a}_1}^\dagger \rangle = \Delta$, $\Delta_{j,j+\mathbf{a}_2} = \langle \hat{c}_j^\dagger \hat{c}_{j+\mathbf{a}_2}^\dagger \rangle = -\Delta$, $\Delta_{j,j+\mathbf{a}_3} = \langle \hat{c}_j^\dagger \hat{c}_{j+\mathbf{a}_3}^\dagger \rangle = 0$, where \mathbf{a}_α denotes a vector that connects nearest neighbor i site and $i + \mathbf{a}_\alpha$ site as $\mathbf{a}_1 = \frac{a}{2}(1, \sqrt{3})$, $\mathbf{a}_2 = \frac{a}{2}(1, -\sqrt{3})$, $\mathbf{a}_3 = a(-1, 0)$, $\mathbf{b}_1 = \mathbf{a}_1 - \mathbf{a}_3$, $\mathbf{b}_2 = \mathbf{a}_2 - \mathbf{a}_3$. The lattice constant is defined as $a \equiv 1$ in this paper. In Fig.1(a), along red links, the SC/SF order parameter is finite; while along black links, the SC/SF order parameter is zero. The effective Hamiltonian then

*Corresponding author; Electronic address: spkou@bnu.edu.cn

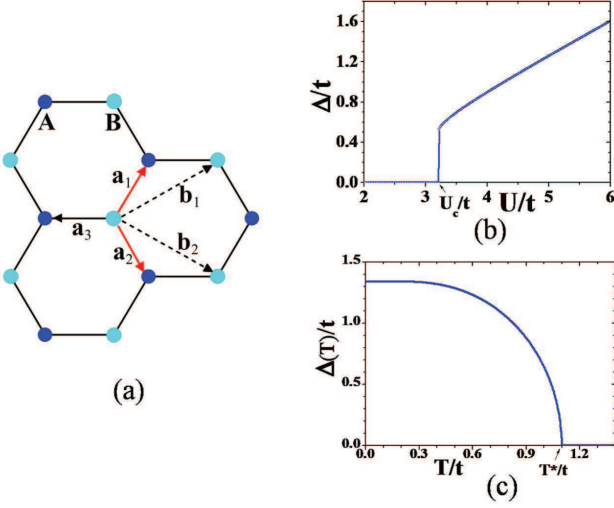


FIG. 1: (a) The illustration of honeycomb lattice of two interpenetrating triangular lattice. A and B denote A and B sublattice. The red links represent the pairing bonds, on which the pairing order parameter is finite; (b) The order parameter Δ vs. the interaction strength U for the case of $t' = 0.01t$ at half-filling; (c) The order parameter Δ vs. the temperature T for the case of $t' = 0.01t$, $U = 5.24t$ at half-filling.

becomes

$$\begin{aligned}
 H_{\text{eff}} = & -t \sum_{\langle ij \rangle} \hat{c}_i^\dagger \hat{c}_j - t' \sum_{\langle\langle ij \rangle\rangle} \hat{c}_i^\dagger \hat{c}_j - \sum_{j \in B} \Delta_{j, j+\mathbf{a}_1} \hat{c}_j^\dagger \hat{c}_{j+\mathbf{a}_1}^\dagger \\
 & - \sum_{j \in B} \Delta_{j, j+\mathbf{a}_2} \hat{c}_{j+\mathbf{a}_2}^\dagger \hat{c}_j^\dagger + h.c. - \mu \sum_i \hat{c}_i^\dagger \hat{c}_i - U \sum_i \hat{n}_i \hat{n}_{i+\mathbf{a}_3}.
 \end{aligned} \quad (2)$$

At zero temperature, there exists a first order phase transition between semi-metal and the SC/SF phase, where $U_c \simeq 3.23t$ when $t' = 0.01t$ at half filling as shown in Fig.1(b). In weakly interaction region, $U < U_c$, the ground state is a semi-metal. When the interaction strength is larger than U_c , in the region of $3.23t \leq U \leq 7.12t$, the ground state turns into a p-wave SC/SF state. In the following parts, we focus on the case of $U = 5.24t$, of which the SC/SF order parameter $\Delta \simeq 1.34t$ at zero temperature. As the temperature increases, the order parameter decreases until it disappears at the critical temperature $T^* = 1.10t$ that corresponds to breaking the Cooper pairing. The order parameter Δ versus temperature T is plotted in Fig.1(c) for the case of $t' = 0.01t$, $U = 5.24t$ at half-filling.

For the p-wave SC/SF on honeycomb lattice, there exists an energy gap for the Bogliubov quasi-particles. For example, for the case of $U = 5.24t$, the energy gap ΔE_g is about $2.0t$. Remember that for the p-wave (p_x -wave or p_y -wave) SC/SF state on a square lattice, the spectrum of quasi-particles is always gapless. And it is obvious that this p-wave SC/SF on honeycomb lattice is not a "topologically ordered" SC/SF. However, there exist Majorana edge states. Now we consider the effective

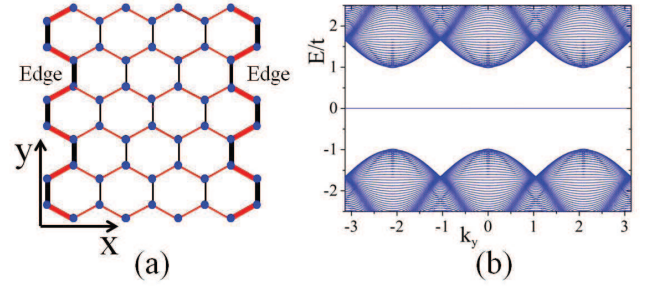


FIG. 2: (Color online) Edge states of p-wave SC/SF on honeycomb lattice for the system with armchair open boundary. The parameters are chosen as $\Delta = 1.34t$, $t' = 0.01t$, $\mu = 0.0136t$. Along red links, the SC/SF order parameter is finite; while along black links, the SC/SF order parameter is zero.

Hamiltonian in Eq.(2) under periodic boundary condition along y-direction and opened boundary condition (armchair boundary) along x-direction (the axis is defined in Fig.2(a)). Now the p-wave SC/SF on a honeycomb lattice behaves like coupled 1D p-wave SC/SFs along x-direction, where the dangling Majorana fermions exist at the boundary[16]. Fig.2 shows the numerical results of the edge states for the case of $\Delta = 1.34t$, $t' = 0.01t$, $\mu = 0.0136t$. From Fig.2, one can see that the Majorana edge states always have a flat-band without hybridizing with each other.

Majorana zero modes around vacancies: Now we study the properties of a lattice defect for the p-wave SC/SF on honeycomb lattice in the presence of an on-site potential at site i_0 , $H_{\text{eff}} \rightarrow H_{\text{eff}} + V_{i_0} \hat{c}_{i_0}^\dagger \hat{c}_{i_0}$. After solving the Bogolubov-de Gennes (BdG) equations with a single lattice defect on a 50×50 lattice with periodic boundary condition, we obtain two localized wave-function with energy $\pm \varepsilon$ around the lattice defect. In the unitary limit, the lattice defect becomes a vacancy shown in Fig.3(a), of which we have an infinite on-site potential, i.e., $V_{i_0} \rightarrow \infty$. For the system with the particle-hole symmetry, $\mu = 0$, $t' = 0$, two localized states turn into a pair of Majorana modes with exact zero energy[15], one Majorana mode at the left side of the vacancy, and the other at the right side. See the results in Fig.3(a): there are two Majorana modes, γ_a, γ_b . Away from the unitary limit, we have a finite on-site potential. As shown in Fig.3(b), the energy levels of the two localized modes versus potential energy V_{i_0} is plotted. From Fig.3(b), we find that as $V_{i_0} \rightarrow \infty$, the energy of the localized state turns into zero.

Next, we consider the case of a line of lattice-defect with multi-vacancy along the SC/SF pairing direction as shown in Fig.4(a). Now the Hamiltonian becomes $H_{\text{eff}} \rightarrow H_{\text{eff}} + \sum_{k=1}^N V_{i_k} \hat{c}_{i_k}^\dagger \hat{c}_{i_k}$. By numerical calculations on a 50×50 lattice, from Fig.4(a), we find that there also exist two Majorana modes localized at both ends of the line-defect, γ_a, γ_b . Now, the end of a line-defect can be considered as the boundary of 1D p-wave SF. Thus

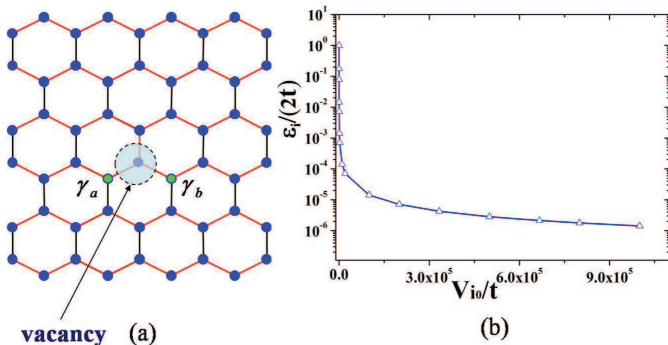


FIG. 3: (a) The lattice vacancy is represented by shaded-dashed-circle, and two green dots denote the two Majorana modes γ_a, γ_b . Along red links, the SC/SF order parameter is finite; while along black links, the SC/SF order parameter is zero. (b) Half of the energy splitting ε_i/t versus on-site potential V_{i0}/t . The detailed explicit Hamiltonian form is shown in Eq.(2). Related parameters are chosen as $\Delta = 1.34t$, $t' = 0, \mu = 0$ at zero temperature.

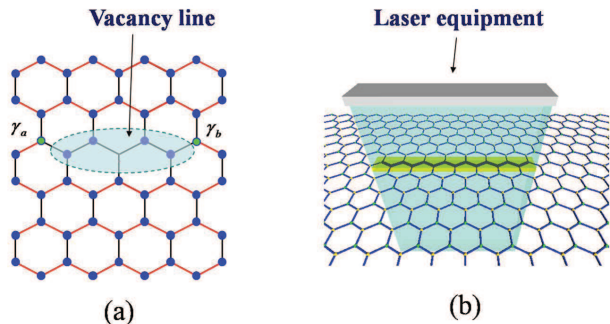


FIG. 4: (a) The illustration of a line-defect. Two Majorana modes γ_a, γ_b are denoted by green dots are localized at ends of the line-defect. (b) The illustration of line-defect created by an addressing line-laser in optical lattice. Along red links, the SC/SF order parameter is finite; while along black links, the SC/SF order parameter is zero.

each end of the line-defect traps a dangling Majorana zero mode. When the line-defect is long enough, the two Majorana modes decouple and have zero energy.

Universal Majorana Fermionic Quantum Computation: Then we consider the couplings between Majorana zero modes of vacancy-lines. For a general case, the universal Hamiltonian of Majorana zero modes is given by

$$H_{\text{Majoran}} = i \sum_i J_i \gamma_{ia} \gamma_{ib} + i \sum_{\langle ij \rangle} J_{ij}^{(2)} \gamma_{ib} \gamma_{ja} \quad (3)$$

$$+ \sum_{\langle i,j \rangle} J_{ij}^{(4)} \gamma_{ia} \gamma_{ja} \gamma_{ib} \gamma_{jb},$$

where J_i denotes the coupling between two Majorana modes of a line-defect i , $J_{ij}^{(2)}$ denotes the coupling between two Majorana modes of two different line-defects i, j , and $J_{ij}^{(4)}$ denotes the strength of the four-Majorana

particle interaction of two different line-defects i, j . γ_{ia} denotes a Majorana fermion at the left side of a line-defect i and γ_{ib} denotes a Majorana fermion at the right side of a line-defect i .

Therefore, the two Majorana modes (γ_{ia}, γ_{ib}) of a line-defect form a physical fermion's parity qubit, $|0\rangle_i$ (quantum state with even fermion's parity) and $c_i^\dagger |0\rangle_i = |1\rangle_i$ (quantum state with odd fermion's parity), respectively. We label a pair of Majorana edge states (γ_{ia}, γ_{ib}) by a complex fermion as $\gamma_{ia} = (c_i + c_i^\dagger)$, $\gamma_{ib} = -i(c_i - c_i^\dagger)$. By representing the Majorana fermions into complex fermions, the universal Hamiltonian in Eq.(3) of coupled Majorana zero modes becomes

$$H_{\text{Majoran}} = \sum_i J_i (2c_i^\dagger c_i - 1) \quad (4)$$

$$+ \sum_{\langle ij \rangle} J_{ij}^{(2)} (c_i c_j^\dagger - c_i^\dagger c_j + c_i c_j - c_i^\dagger c_j^\dagger)$$

$$- \sum_{\langle i,j \rangle} J_{ij}^{(4)} (2c_i^\dagger c_i - 1) (2c_j^\dagger c_j - 1).$$

We firstly calculate J_i , the coupling between two Majorana fermions at the ends of a single lattice defect (a shortest line-defect with a defect). In the unitary limit, we have two degenerate zero modes (γ_{ia}, γ_{ib}) around the lattice defect for the SC/SF with particle-hole symmetry ($\mu = 0, t' = 0$). Away from the unitary limit of the SC/SF, $V_0 \neq \infty$, we have the finite energy splitting of the Majorana modes as $\varepsilon_i \neq 0$. Then we can identify half of the energy splitting $\varepsilon_i/2$ to be the coupling between two Majorana modes around this lattice defect as $J_i \equiv \varepsilon_i/2$. When the energy splitting $\varepsilon_i > 0$ (< 0), the system energetically favors the empty (occupied) state. We also calculate the energy splitting of two Majorana fermions of a line-defect with multi-defect (the number of the defect is more than two) and found that the energy splitting of the two Majorana modes is always zero. In this sense from Fig.3(b), to tune the coupling J_i (that is $\varepsilon_i/2$) of a line-defect between two Majorana modes (γ_{ia}, γ_{ib}), we can first shrink the line-defect into a single vacancy and then change the on-site potential V_0 from infinite to a finite value.

Next we calculate $J_{ij}^{(2)}$, the coupling between two Majorana modes at the ends of two different line-defects. Now we consider two line-defects as shown in Fig.5(a). When two line-defects are well separated, we have four Majorana modes $\gamma_{ia}, \gamma_{ib}, \gamma_{ja}, \gamma_{jb}$ with exact zero energy. Now we move the two line-defects nearby. The wavefunctions of the two Majorana zero modes γ_{ib}, γ_{ja} will overlap and give rise to a small energy splitting ΔE_{ij} from exact zero energy level. The tunneling splitting ΔE_{ij} is about $J_{ij}^{(2)} \propto e^{-\Delta E_0 L_{i,j}}$ where $L_{i,j}$ is the distance between right-site of i -th line-defect and left-site of the j -th line-defect. In Fig.5(b), we plot the results of $J_{ij}^{(2)}$ versus $L_{i,j}$ for the case of $t' = 0.01t, \mu = 0.013t$. For this case $L_{i,j} \gg a$, we get zero tunneling ampli-

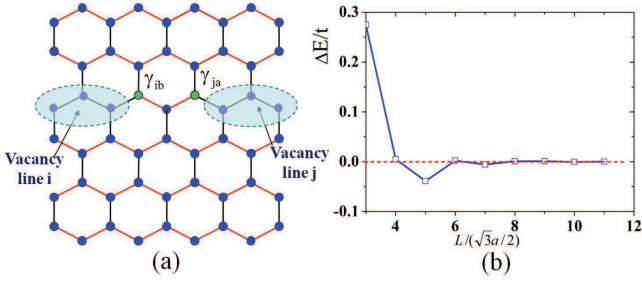


FIG. 5: (a) The illustration of two line-defects. The two Majorana fermions γ_{ia}, γ_{ib} are denoted by the green dots that localize at ends of the line-defect 1 and the line-defect 2, respectively. (b) The energy splitting $\Delta E/t$ versus the distance between the ends of two line-defects as shown in (a). The parameters are chosen as $\Delta = 1.34t$, $t' = 0.01t$, $\mu = 0.013t$. Along red links, the SC/SF order parameter is finite; while along black links, the SC/SF order parameter is zero.

tude as $J_{i,j} \rightarrow 0$. In this sense, to tune the coupling $J_{ij}^{(2)}$ (that is ΔE_{ij}) of two line-defects between two Majorana modes (γ_{ib}, γ_{ja}), we can just change the distance of two line-defects.

Thirdly we calculate the strength of four-Majorana particle interaction $J_{ij}^{(4)}$ between the four Majorana modes $\gamma_{ia}, \gamma_{ib}, \gamma_{ja}, \gamma_{jb}$ around two line-defects. Here we also consider two line-defects in the unitary limit. When two line-defects are well separated, there is no four-Majorana particle interaction at all. When two line-defects are nearby, the four-Majorana particle interaction could be induced by the nearest neighbor attractive interaction along un-pairing direction as $-U \sum_i \hat{n}_i \hat{n}_{i+\mathbf{a}_3}$. As shown by Fig.6, there are four Majorana fermions around the two line-defects $\gamma_{ia}, \gamma_{ib}, \gamma_{i+\mathbf{a}_3,a}, \gamma_{i+\mathbf{a}_3,b}$. The two zero modes γ_{ia}, γ_{ib} form a complex fermion c_i by the definition $\gamma_{ia} = (c_i + c_i^\dagger)$, $\gamma_{ib} = -i(c_i - c_i^\dagger)$ and the other two zero modes $\gamma_{i+\mathbf{a}_3,a}, \gamma_{i+\mathbf{a}_3,b}$ form another complex fermion c_j by the definition $\gamma_{i+\mathbf{a}_3,a} = (c_{i+\mathbf{a}_3} + c_{i+\mathbf{a}_3}^\dagger)$, $\gamma_{i+\mathbf{a}_3,b} = -i(c_{i+\mathbf{a}_3} - c_{i+\mathbf{a}_3}^\dagger)$. Then after considering the nearest neighbor attractive interaction $-U \sum_i \hat{n}_i \hat{n}_{i+\mathbf{a}_3}$, we will get residue interaction term between the two complex fermions ($c_i, c_{i+\mathbf{a}_3}$). For this case, the strength of the four-Majorana particle interaction term is given by

$$\begin{aligned}
 -J_{i,i+\mathbf{a}_3}^{(4)} &= \sum_i \psi_i^\dagger \psi_{i+\mathbf{a}_3}^\dagger (H_{\text{eff}}) \psi_i \psi_{i+\mathbf{a}_3} \\
 &= \sum_i \psi_i^\dagger \psi_{i+\mathbf{a}_3}^\dagger (-U \hat{n}_i \hat{n}_{i+\mathbf{a}_3}) \psi_i \psi_{i+\mathbf{a}_3} \rightarrow -\frac{U}{4}.
 \end{aligned} \tag{5}$$

In this sense, to tune the four-Majorana particle interaction $J_{ij}^{(4)}$ of two line-defects between four Majorana modes ($\gamma_{ia}, \gamma_{ib}, \gamma_{ja}, \gamma_{jb}$), we can just move two parallel line-defects nearby. However, for this case, the two-Majorana couplings between ($\gamma_{ia}, \gamma_{i+\mathbf{a}_3,a}$) and ($\gamma_{ib},$

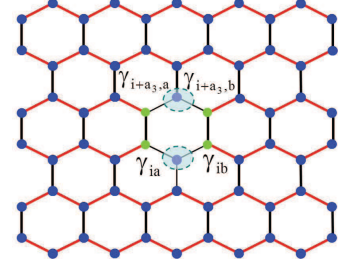


FIG. 6: The illustration of four Majorana modes induced by two defects that can combine into two complex fermions ($c_i, c_{i+\mathbf{a}_3}$). Along red links, the SC/SF order parameter is finite; while along black links, the SC/SF order parameter is zero.

$\gamma_{i+\mathbf{a}_3,b}$) are still finite, $J_{i,i+\mathbf{a}_3}^{(2)} \simeq t \neq 0$.

By freely tuning all terms in Eq.(4), we may make the following two universal gate set in fermionic quantum computation (up to phase factor) as $e^{\frac{\pi}{8}\gamma_i \gamma_j}$ and $e^{i\frac{\pi}{4}\gamma_1 \gamma_2 \gamma_3 \gamma_4}$ [1]: 1) To design $e^{\frac{\pi}{8}\gamma_{ia} \gamma_{ib}}$ gate we can shrink the line-defect into a single vacancy and then fix the on-site potential V_0 under a given time-period as $\Delta t = \frac{\pi \hbar}{8J_{ij}(V_0)}$; 2) To design $e^{\frac{\pi}{8}\gamma_{ib} \gamma_{ja}}$ gate we can control the given two line-defects nearby under fixed time-period as $\Delta t = \frac{\pi \hbar}{8J_{ij}^{(2)}(L_{i,j})}$; 3) To design $e^{i\frac{\pi}{4}\gamma_{ia} \gamma_{ib} \gamma_{i+\mathbf{a}_3,a} \gamma_{i+\mathbf{a}_3,b}}$ gate we can control the given two line-defects nearby under fixed time-period as $\Delta t = \frac{\pi \hbar}{4J_{i,i+\mathbf{a}_3}^{(4)}}[22]$. Thus, in principle, people are capable of doing arbitrary unitary transformation on the protected subspace by controlling the vacancies.

Errors: For the p-wave SF on honeycomb lattice, one always has a large energy gap ΔE_g for the fermions and a very tiny energy splitting ΔE of the nearly-degenerate Majorana modes, i.e., $\Delta E \ll \Delta E_g$. Based on this condition ($\Delta E \ll \Delta E_g$), we may ignore the excited states with $E > \Delta E_g$ and consider only the Majorana modes as the protected sub-space. In this sense, we must consider the case at fairly low temperature $k_B T \ll \Delta E_g$. Now there exist few excited quasi-particles, $n_f \sim e^{-\Delta E_g/k_B T}$. In addition, the random local potentials will lead to the energy splitting of the Majorana modes. Thus when we move the vacancies nearby to do unitary operations, the random energies of the Majorana modes will lead to errors. By numerical calculations, we find that the energy splitting by random potential is very tiny. So we may ignore this type of errors.

To store quantum information by the Majorana zero modes of the line-defect, we must use a long line-defect to separate the Majorana modes. Thus, the distance between two Majorana modes are set to be much bigger than lattice distance a as $\min L_{i,j} \gg a$. For this case, we get zero tunneling amplitude as $J_{ij}^{(2)}(L_{i,j}) \rightarrow 0$. Now the system truly immune to decoherence.

Possible realization in cold atoms: Now we propose an experiment scheme for the realization of the spinless fermion model on a honeycomb lattice with near-

est attractive interaction given in Eq.(1). To realize this model, a Bose-Fermi mixture on optical honeycomb lattice of cold atoms may be a possible candidate. As given in Ref.[23], the bosons with unit filling form a Mott insulator and the spinless fermions with half filling form a semi-metal. When the on-site repulsive interaction between bosons and fermions U_{bf} is larger than boson-boson repulsion U_{bb} i.e., $U_{bf} > U_{bb}$, a spinless fermion and a bosonic hole bind into a composite spinless fermion created by $\hat{c}^\dagger = \hat{f}^\dagger \hat{b}$, with \hat{f}^\dagger , \hat{b} being the fermionic creation and the bosonic annihilation operators, respectively. The effective nearest attraction is given by $U/t = 2(U_{bf}/U_{bb} - 1)$, and the effective nearest (next nearest) hopping $t = 2t_{bf}^2/U_{bf}$ ($t' = 2t'_{bf}{}^2/U_{bf}$), where t_{bf} (t'_{bf}) denotes the tunneling strength for the bosons and fermions of the hopping between the nearest (next nearest neighbor) neighbor lattices (here we have supposed that $t_b = t_f = t_{bf}$, $t'_b = t'_f = t'_{bf}$ for simplicity). See detailed calculations in the supplementary materials. In experiment, for example, ^{171}Yb - ^{174}Yb or ^6Li - ^7Li mixture, the nearest neighbor effective attracting interaction U may be tuned employing well-characterized homonuclear and heteronuclear Feshbach resonances[24-26]. Thus in cold atom system, people have ability to tune the parameters in Eq.(1) including t'/t , U/t .

On the other hand, recently, in cold atoms people have made great progress on the manipulation of a single atom on an optical lattice[27-29]. A tightly focused

dimple laser beam with an accuracy about $0.1a$ can be applied onto individual lattice sites to generate a vacancy in the optical lattice or line-vacancy[27-29]. By moving the addressing laser beam as shown in Fig.4(b) from one site to another, people are able to accurately manipulate the position and the length of a line-defect on a two-dimensional optical lattice. Therefore two dimensional ultracold atomic Fermi gases provide an ideal platform for creating and manipulating Majorana fermions.

Conclusion: We have proposed a feasible scheme towards designing a quantum computer, which incorporates intrinsic fault tolerance by controlling the Majorana fermions accurately via controlling addressing laser beams on optical lattice. In particular, we find that the lattice defects here plays the role of a Majorana fermion. Therefore, by creating and manipulating lattice defects accurately via addressing laser beams, we can do quantum computation fully optically. So we call this approach "Majorana-fermionic quantum computation" to emphasize the difference between the topological quantum computation by braiding non-Abelian anyons.

Acknowledgments

This work is supported by NFSC Grant No. 11174035, National Basic Research Program of China (973 Program) under the grant No. 2011CB921803, 2012CB921704.

-
- [1] S. B. Bravyi, and A. Yu. Kitaev, *Annals of Physics* **298**, 210-226 (2002).
 - [2] A. Kitaev, *Ann. Phys.* **303**, 2-30 (2003).
 - [3] L. B. Ioffe, et al, *Nature* **415**, 503-506 (2002).
 - [4] S. P. Kou, *Phys. Rev. Lett.* **102**, 120402-4 (2009).
 - [5] A. Kitaev, *Ann. Phys.* **321**, 2-111 (2006).
 - [6] C. Nayak, S. H. Simon, A. Stern, M. Freedman, and S. Das Sarma, *Rev. Mod. Phys.* **80**, 1083-1159 (2008).
 - [7] M. Freedman, M. Larsen, and Z. Wang, *Math. Phys.* **227**, 605-622 (2002).
 - [8] S. Das Sarma, M. Freedman, and C. Nayak, *Phys. Rev. Lett.* **94**, 166802-4 (2005).
 - [9] L. S. Georgiev, *Phys. Rev. B* **74**, 235112 (2006). L. S. Georgiev, *Nucl. Phys. B* **789**, 552-590 (2008).
 - [10] J. Eisenstein, K. Cooper, L. Pfeiffer and K West, *Phys. Rev. Lett.* **88**, 076801 (2002).
 - [11] J. Xia, et al. *Phys. Rev. Lett.* **93**, 176809 (2004).
 - [12] S. Das Sarma, C. Nayak, and S. Tewari, *Phys. Rev. B* **73**, 220502 (2006).
 - [13] J. Alice, Y. Oreg, G. Refael, F. von Oppen, and M. P. A. Fisher, *Nature Physics* **7**, 412 (2011).
 - [14] L. Fu, and C. L. Kane, *Phys. Rev. Lett.* **100**, 096407 (2008).
 - [15] Jing He, Ying-Xue Zhu, Ya-Jie Wu, Lan-Feng Liu, Ying Liang, Su-Peng Kou, *Phys. Rev. B* **87**, 075126 (2013).
 - [16] A. Yu. Kitaev, *Physics Uspekhi*, **44**, 131 (2001).
 - [17] D. Poletti, C. Miniatura, and B. Grémaud, *EPL*, **93** 37008 (2011).
 - [18] M. Greiner, O. Mandel, T. Esslinger, T. W. Hänsch, and I. Bloch, *Nature* **415**, 39-44 (2002).
 - [19] D. Jaksch, C. Bruder, J. I. Cirac, C. W. Gardiner, and P. Zoller, *Phys. Rev. Lett.* **81**, 3108 (1998).
 - [20] M. J. Bijlsma, B. A. Heringa, and H. T. C. Stoof, *Phys. Rev. A* **61**, 053601 (2000).
 - [21] M. Lewenstein, A. Sanpera, V. Ahufinge, B. Damski, A. Sen(De), and U. Sen, *Advances in Physics* **56**, 243-379 (2007).
 - [22] To eliminate the effects of the two-Majorana couplings between $(\gamma_{ia}, \gamma_{i+\mathbf{a}_3, a})$ and $(\gamma_{ib}, \gamma_{i+\mathbf{a}_3, b})$, after doing the $e^{i\frac{\pi}{4}\gamma_{ia}\gamma_{ib}\gamma_{i+\mathbf{a}_3, a}\gamma_{i+\mathbf{a}_3, b}}$ gate, we must do another two operations, $e^{\frac{\pi}{4}\gamma_{ia}\gamma_{i+\mathbf{a}_3, a}}$ gate and $e^{\frac{\pi}{4}\gamma_{ib}\gamma_{i+\mathbf{a}_3, b}}$ gate.
 - [23] M. Lewenstein et al., *Phys. Rev. Lett.* **92**, 050401 (2004).
 - [24] T. Köhler and K. Góral, and Paul S. Julienne, *Rev. Mod. Phys.* **78**, 1311-1361 (2006).
 - [25] M. Kitagawa et al., *Phys. Rev. A* **77**, 012719 (2008).
 - [26] E. G. M. v. Kempen, B. Marcelis, and S. J. J. M. F. Kokkelmans, *Phys. Rev. A* **70**, 050701(R) (2004).
 - [27] N. Gemelke, Xibo Zhang, Chen-Lung Hung & Cheng Chin, *Nature* **460**, 995-998 (2009).
 - [28] Jacob F. Sherson, et al, *Nature* **467**, 68-72 (2010).
 - [29] C. Weitenberg, et al, *Nature* **471**, 319-324 (2011).